



## OPEN

SUBJECT AREAS:  
ELECTRON MICROSCOPY  
BIOOCEANOGRAPHY  
BIOMINERALIZATION

Received  
20 March 2014

Accepted  
28 July 2014

Published  
22 August 2014

Correspondence and  
requests for materials  
should be addressed to  
M.A.R. (mazizur.  
rahman@utoronto.ca;  
azizur31@yahoo.  
com)

# First evidence of chitin in calcified coralline algae: new insights into the calcification process of *Clathromorphum compactum*

M. Azizur Rahman & Jochen Halfar

Department of Chemical & Physical Sciences, University of Toronto at Mississauga, Ontario, Canada.

Interest in calcifying coralline algae has been increasing over the past years due to the discovery of extensive coralline algal dominated ecosystems in Arctic and Subarctic latitudes, their projected sensitivity to ocean acidification and their utility as palaeoenvironmental proxies. Thus, it is crucial to obtain a detailed understanding of their calcification process. We here extracted calcified skeletal organic matrix components including soluble and insoluble fractions from the widely-distributed Subarctic and Arctic coralline alga *Clathromorphum compactum*. The lyophilized skeletal organic matrix fractions showed comparatively high concentrations of soluble and insoluble organic matrices comprising 0.9% and 4.5% of skeletal weight, respectively. This is significantly higher than in other skeletal marine calcifiers. Attenuated Total Reflection-Fourier Transform Infrared Spectroscopy (ATR-FTIR) and X-Ray Diffraction (XRD) results indicate that chitin is present in the skeletal organic matrices of *C. compactum*. This polymer exhibits similar hierarchical structural organizations with collagen present in the matrix and serves as a template for nucleation and controls the location and orientation of mineral phases. Chitin contributes to significantly increasing skeletal strength, making *C. compactum* highly adapted for living in a shallow high-latitude benthic environment. Furthermore, chitin containing polysaccharides can increase resistance of calcifiers to negative effects of ocean acidification.

The involvement of chitin and collagen in marine biomineralization has been described previously<sup>1–4</sup>. However, this is the first report on the identification of chitin in the skeletal structural system of coralline algae. After cellulose, chitin is the second most important natural polymer in the world. Its role in biomineralization is well described, especially in mollusc shells<sup>1,3</sup>, crustaceans<sup>3,5</sup> and sponges<sup>3,4</sup>. Chitin can also be enzymatically deacetylated to chitosan, a more flexible and soluble polymer<sup>2,5,6</sup>. Both chitin and collagen are usually formed as extracellular secretions, which eventually deposit crystalline minerals<sup>3</sup>. In natural extracellular matrices, proteoglycans and glycosaminoglycans have important roles in linking with the fibrous structure of collagen to obtain mechanical stability and compressive strength<sup>7</sup>. Amino groups of chitosan function as binding sites with collagen to improve its stability, without significantly altering the chemical characteristics of both polymers<sup>3,7,8</sup>. Therefore, it might be important to develop collagen composites with chitosan to create more suitable biomimetic microenvironments for cells.

Chitin is the main component of cell walls found in plants, bacteria, fungi<sup>9,10</sup>, which is composed mostly of glycoprotein<sup>11</sup>. Like plants, algae have cell walls<sup>10,12</sup>. Algal cell walls contain either polysaccharides that we found in our present study or a variety of glycoproteins (unpublished observation) or both.

Coralline algae are among the calcifying organisms that appear to be the most sensitive to ocean acidification<sup>13–18</sup> due to the solubility of their high magnesium calcite skeletons<sup>19</sup>. Coralline algae are used as paleoenvironmental proxies because of their clearly defined growth information archived in annual growth bands<sup>20–25</sup>, widespread distribution, and multicentury-long life spans. Coralline algae are abundant from tropical to polar oceans, sometimes covering up to 100% of the shallow seafloor<sup>26,27</sup>. However, a great deal remains unknown about the CaCO<sub>3</sub> formation in the algal skeletons and the mechanism of growth, especially regarding the key components of organic molecules in the biomineralization process. Therefore, we studied the coralline alga *Clathromorphum compactum* to understand the skeletal structural system and explore the functional molecules in the biomineralization process by which the skeletal minerals form in this species (see Fig. 1).

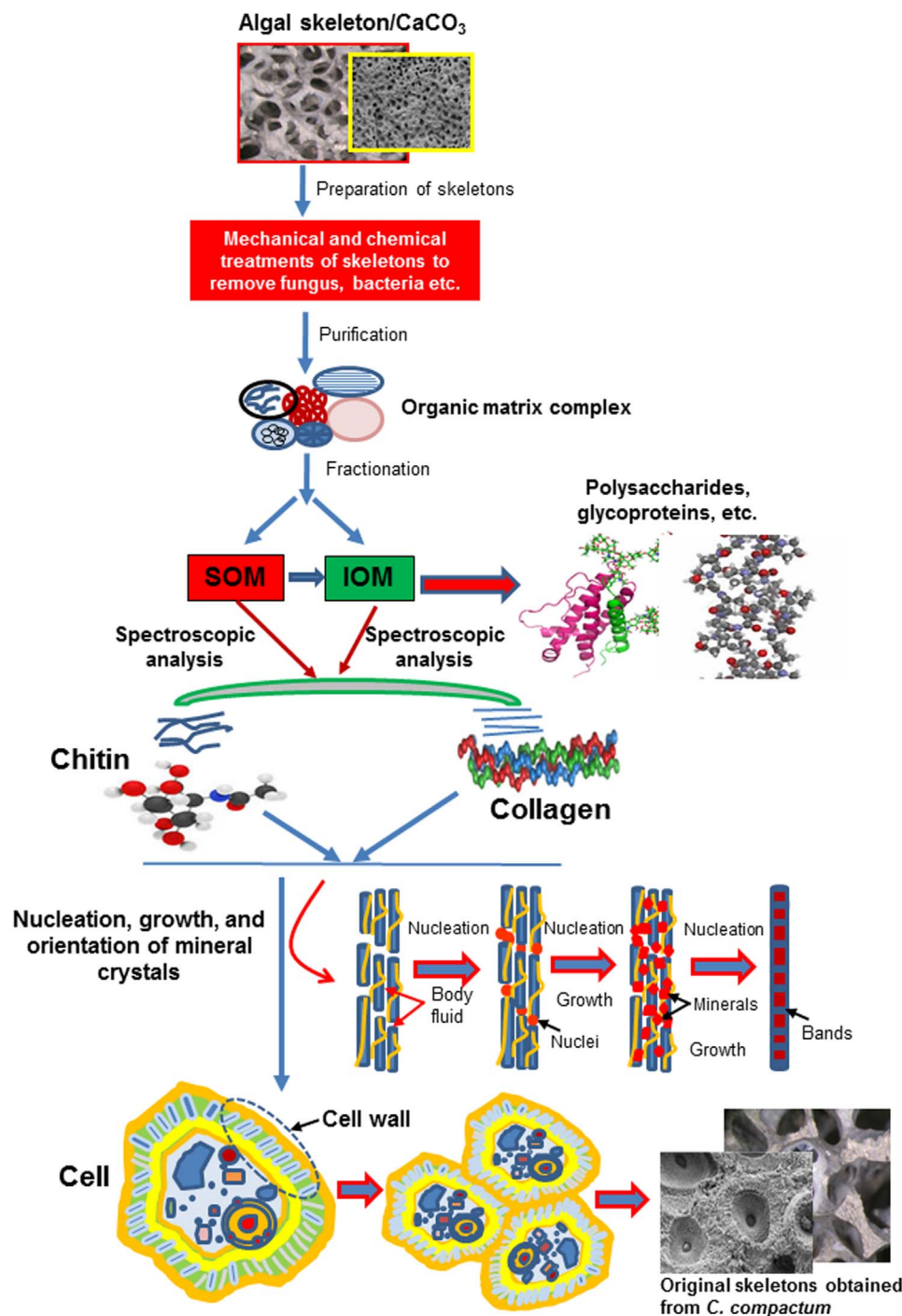


**Figure 1** | Schematic approach in understanding the dynamic mechanism of calcification, purification of the organic matrix components and the nucleation, growth, and orientation of mineral crystals by the chitin and collagen matrices at different stages of mineralization in the algal skeletons.

## Methods

**Experimental specimens.** Samples of *C. compactum* were live collected in 2008 at 10 m depth near Quirpon, Newfoundland, Canada (51°35.135' 55°25.490'), and Bay Bulls, Newfoundland, Canada (47°18.496' 52°47.354'). Specimens from Bay Bulls were kept alive in a mesocosm with artificial seawater for one year before being flash frozen at −30°C. Frozen specimens were thawed immediately prior to processing. Algae were maintained in a mesocosm setting for calibration purposes using light and temperature conditions reflecting the natural environment at their site of collection before being frozen at −30°C. Freezing was done to prevent contamination by bacteria or fungi prior to analysis. For this study only portions of the algal skeleton that had formed prior to field collection were analyzed in order to avoid sampling skeletal material formed during the mesocosm experiment.

**Preparation of skeletons.** To avoid contamination by other associated tissues (e.g., fungus, bacteria etc.) and unwanted substances, the preparation of skeletons from the

algal body must be performed carefully. To do so, we used a series of mechanical and chemical treatments. (1) The selected skeletons were finely ground; (2) All pieces were washed with 95% ethanol (five times) and distilled water (ten times) while stirring; (3) The skeletons were dried and examined using a microscope to determine whether they were completely free of unwanted tissues and other contaminants. We also confirmed via Scanning electron microscope (SEM) that all skeletons are completely contamination-free; (4) Skeletal powder was stirred with 1 M NaOH for 2 h; (5) To ensure again that the skeletons were tissue free (especially fungus and bacteria), they were stirred vigorously in a 10% sodium hypochlorite (NaOCl) bleaching solution for 1 h to remove fleshy tissues and debris. The treated samples were washed under distilled water until all chemicals were removed. Finally, the samples were washed with MilliQ water five times. All steps in the preparation of skeletons were conducted at room temperature, and the materials obtained were stored at 4°C until further analysis.

We also successfully purified algal proteins (paper in preparation) from the same samples used for the present study (both soluble and insoluble organic matrices),



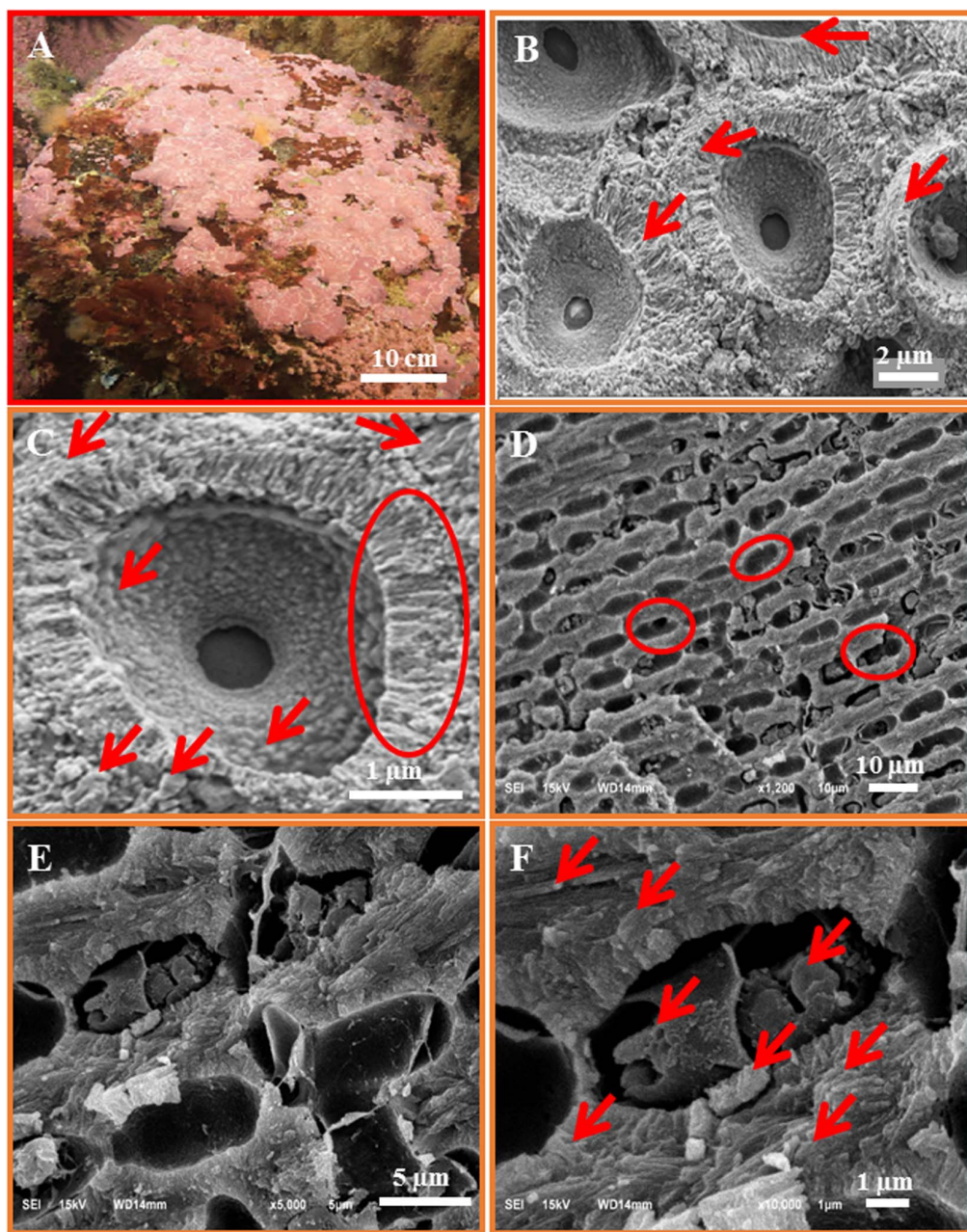


**Figure 2 | Observation of the algal skeletal structure.** (A) Living specimen of crustose coralline alga *C. compactum*<sup>12</sup> (B) SEM image of the structural shape of the cells with their cell walls (red arrows) and coarse  $\text{CaCO}_3$  crystals. (C) SEM of an enlarged view of a cell in the skeleton. (D) SEM view of the cells from a fractured live-collected specimen. (E) SEM shows the  $\text{CaCO}_3$  deposition and crystal faces on the fractured samples (enlarged view from D) (F) SEM of an enlarged view (from E) of fractured sample showing magnesium calcite crystals [rhombohedra (104)] with different faces in cell, cell wall and outside the wall (arrows).

which provides additional evidence that samples were contamination-free. In molecular studies, proteins can only be obtained from completely purified organisms.

**Preparation of Soluble and Insoluble Organic Matrices.** The mechanically and chemically cleaned alga (ca. 10 g) were decalcified in 0.5 M EDTA-4Na (pH 7.8) overnight. The decalcifying solution was centrifuged (Eppendorf-5430) at 4,000 rpm (15 minutes), and the soluble organic matrix (SOM) in the supernatant was filtered and collected for further purification. The insoluble organic matrix (IOM) in the precipitate was subsequently lyophilized and washed with distilled water (5 times). The solution was dialyzed prior to lyophilisation to remove EDTA against  $5 \times 1$  L of distilled water for 64 h while water was changed five times using dialysis tubing. Additional details on sample preparation can be found in Rahman et al.<sup>28,29</sup>

To purify SOM, filtrated samples were passed through two Sep-Pak C18 cartridges connected in tandem (Waters Associates, Milford, MA) to remove the EDTA completely and separate the soluble macromolecules, followed by passing through 10% acetonitrile (2 mL/three times). Finally, the absorbed macromolecules

were eluted in 50% acetonitrile (2 mL/three times), frozen in a deep freezer and lyophilized.

**Infrared (IR) Spectrometry.** Fourier transform infrared spectroscopy (FTIR) analyses were directly performed on finely powdered *C. compactum* skeletal material. Powdered samples of skeletons and KBr (potassium bromide) were mixed (about 5% powdered samples in KBr) and loaded into the sample holder. A background spectrum was measured for KBr.

SOM (soluble organic matrix) and IOM (insoluble organic matrix) have different properties and were therefore prepared differently for analysis by ATR-FTIR to understand the details of structural and functional properties of the skeletal material. Both SOM and IOM were subjected to attenuated total reflection-Fourier transform infrared spectroscopy (ATR-FTIR) using a FTIR spectrometer (Model Alpha, Bruker) equipped with a diamond ATR crystal cell ( $45^\circ$  ZnSe; 80 mm long, 10 mm wide and 4 mm thick). For spectral analysis, the SOM and IOM lyophilized samples were placed onto the crystal cell and the cell was clamped into the mount of the FTIR

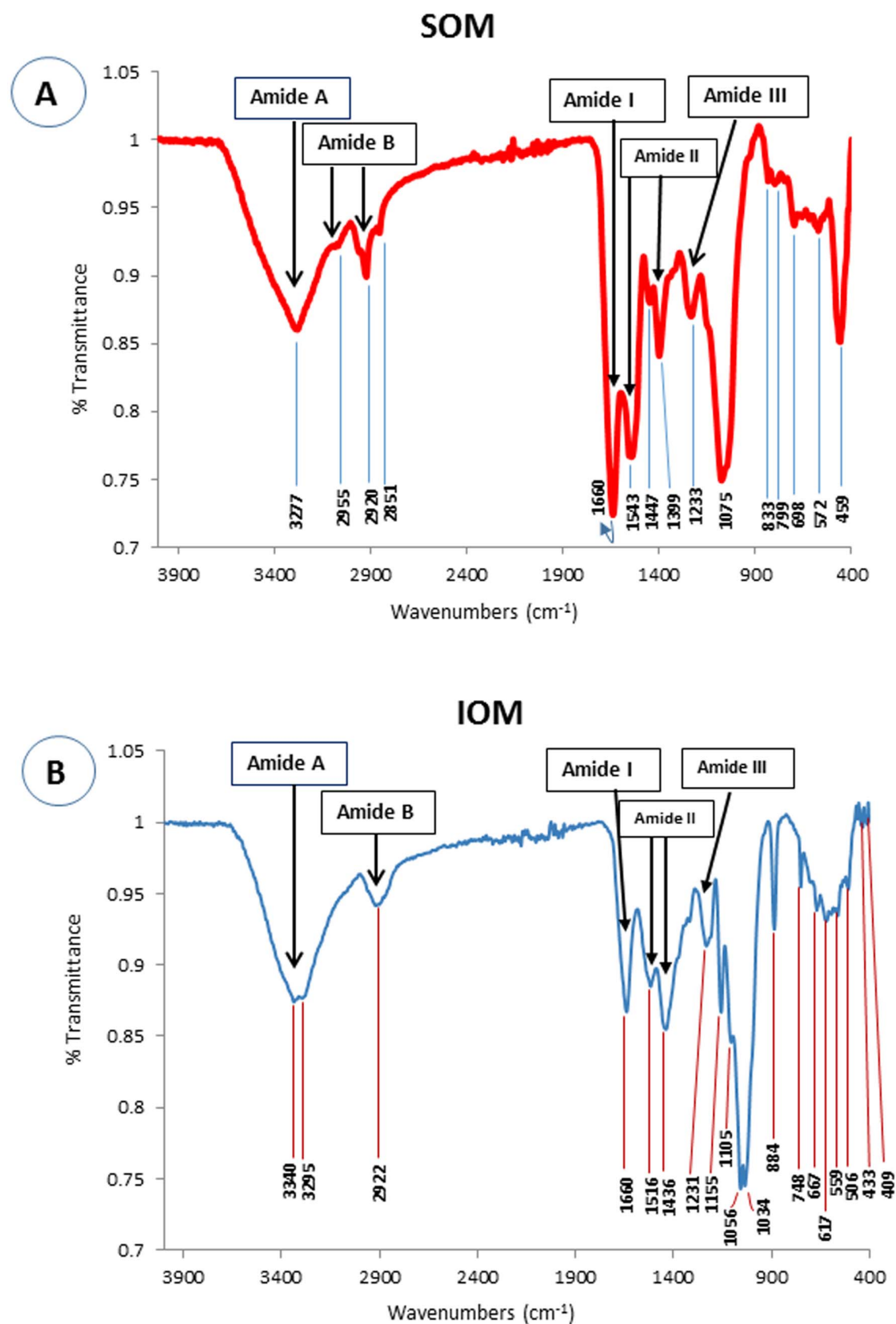


**Figure 3 |** ATR-FTIR spectra of soluble (SOM) and insoluble (IOM) organic matrix extracted from the calcitic skeleton of the coralline alga *C. compactum*. (A) FTIR spectra of skeletal SOM in the range of 4000–400  $\text{cm}^{-1}$  (indicative of chitin). (B) FTIR spectra of skeletal IOM of chitin. Maximum of transmittance bands for both SOM and IOM are indicated.

spectrometer. Spectra in the range of 400–4000  $\text{cm}^{-1}$  with automatic signal gain were collected in 32 scans at a resolution of 4  $\text{cm}^{-1}$  and were rationed against a background spectrum recorded from the clean empty cell.

**X-Ray Diffraction (XRD).** The same finely ground skeletal powder samples as for FTIR were used for this analysis. The polymorphism of crystals in the skeletons was determined by an X-ray diffractometer (Phillips) with 30 kV and 40 mA Cu K $\alpha$ .

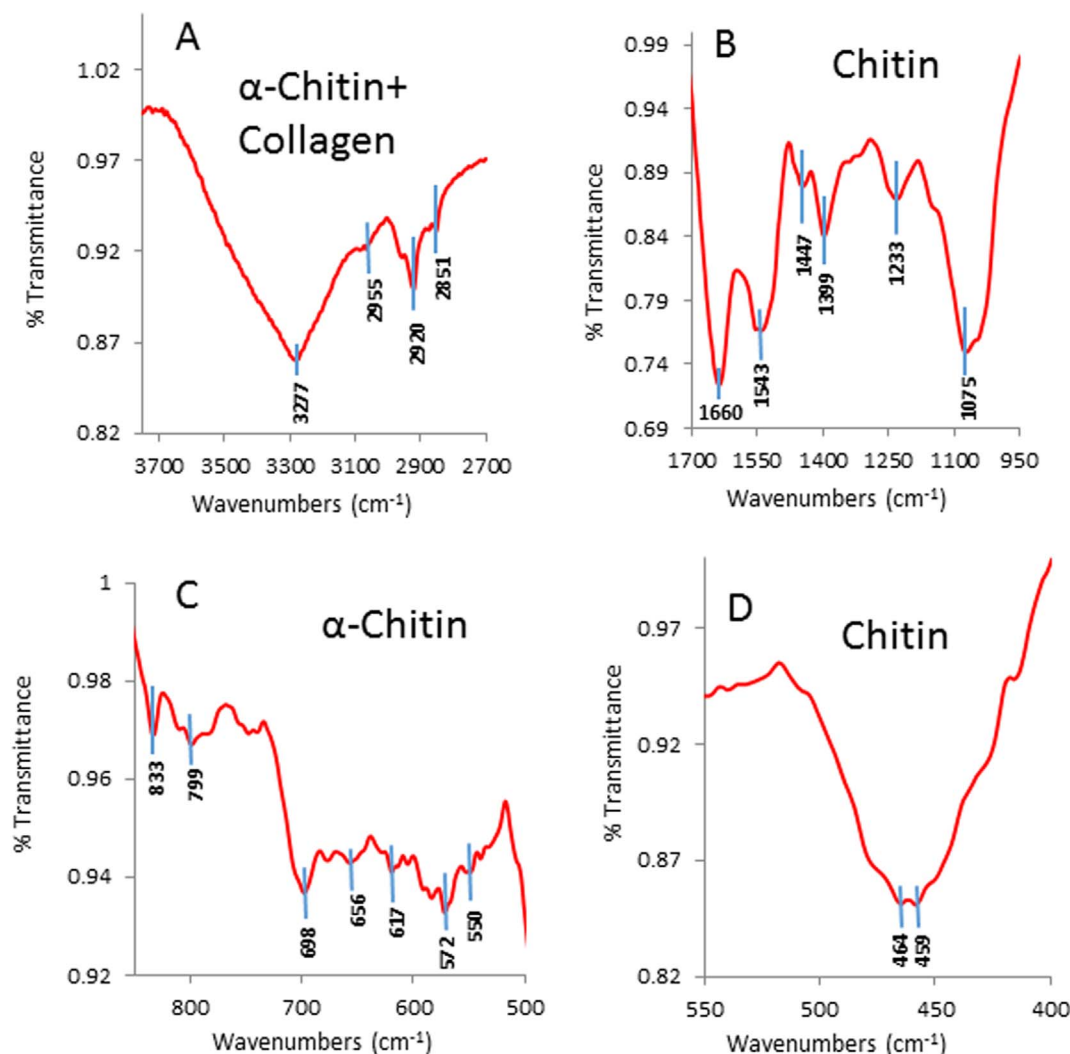


**Figure 4** | ATR-FTIR spectra of chitins in the soluble organic matrix (SOM) fraction.

radiations. Sample analyses were carried out in the  $20^{\circ}$ – $60^{\circ}$  range of  $2\theta$  angle, with step sizes of  $0.020^{\circ}$  and a point measurement time of 2 s.

**Scanning Electron Microscopy (SEM).** In order to understand skeletal structure, *C. compactum* samples were subjected to observation under SEM (JSM6610LV; JEOL operated at 15 kV, WD14 mm). Prior to that samples were treated to remove any contamination as mentioned above (see preparation of skeletons) and SEM observations were made prior to grinding. All specimens were placed in a sample holder and coated with a palladium–gold mixture.

## Results

**Skeletal structure of *C. compactum*.** Scanning electron microscope (SEM) images of the studied species show the microstructural pattern of the cells in the skeletons and the orientation of  $\text{CaCO}_3$  crystals structures (Fig. 2B–D), which were formed biologically by the polysaccharides contained in the organic matrices. As shown in Fig. 2B, SEM reveals the structural shape of the cell walls (red arrows) and coarse  $\text{CaCO}_3$  crystals. An enlarged view of a cell in the skeleton demonstrates the architecture of the cell wall (red box in Fig. 2C) with its crystalline structure (arrows in Fig. 2C). The cells from a fractured piece of *C. compactum* are shown in Fig. 2D (red boxes). Figures 2E, F indicate the orientation of crystal structures on the fractured samples with an enlarged view showing magnesium calcite crystals with different planes (see fig. 9 for details crystal planes in the skeleton of *C. compactum*) in the cell, cell wall and outside the wall.

**IR analyses. Soluble organic matrix (SOM).** The structural and functional properties of the soluble organic matrix were analyzed by ATR-FTIR (Fig. 3A). In an analysis of lyophilized soluble organic matrix (0.9% weight of skeletons) the FTIR showed structural protein amide bands, amide A ( $3000$ – $3500\text{ cm}^{-1}$ ), amide B ( $2800$ – $2990\text{ cm}^{-1}$ ), amide I ( $1600$ – $1700\text{ cm}^{-1}$ ), amide II ( $1300$ – $1590\text{ cm}^{-1}$ ) and amide III ( $1200$ – $1290\text{ cm}^{-1}$ ). The amide bands in SOM also characterize as a collagen scaffold<sup>9</sup>. The main band at  $1660\text{ cm}^{-1}$  is indicative of crystalline chitin formation<sup>30,31</sup> in SOM. The other strong chitin bands at  $3277\text{ cm}^{-1}$  (amide A),  $2920\text{ cm}^{-1}$  (amide B),  $1543$ ,  $1399\text{ cm}^{-1}$  (amide II),  $1233\text{ cm}^{-1}$  were identified in the structural crystalline side of the SOM. A strong band at  $1075\text{ cm}^{-1}$  in the range  $1030$ – $1110\text{ cm}^{-1}$  (stretching  $\text{C}=\text{O}$ ) is also indicative of chitin. All FTIR spectra ( $833$ ,  $799$ ,  $698$ ,  $572\text{ cm}^{-1}$ ) including strong bands at  $459\text{ cm}^{-1}$  in the fingerprint region ( $400$ – $850\text{ cm}^{-1}$ ) showed chitin formation<sup>30</sup>. We divided four regions (A, B, C, D) of IR fractions to clearly understand the findings and axis labels indicating specific peaks for chitin and collagen (Fig. 4). FTIR spectra of chitins for the SOM fraction with each region were recorded separately (Fig. 4). The three bands resolved in the CH stretching region of the SOM IR spectra at  $2955$ ,  $2920$ ,  $2851\text{ cm}^{-1}$  are all characteristics of  $\alpha$ -chitin (Fig. 4A)<sup>31</sup> and a collagen scaffold<sup>9</sup>. The fingerprint region of the IR spectrum at  $698\text{ cm}^{-1}$  also points to  $\alpha$ -chitin (Fig. 4C)<sup>30</sup>.

**Insoluble organic matrix (IOM).** There is a very high concentration (4.5% weight of skeleton) of IOM. To analyse the IOM, ATR-FTIR



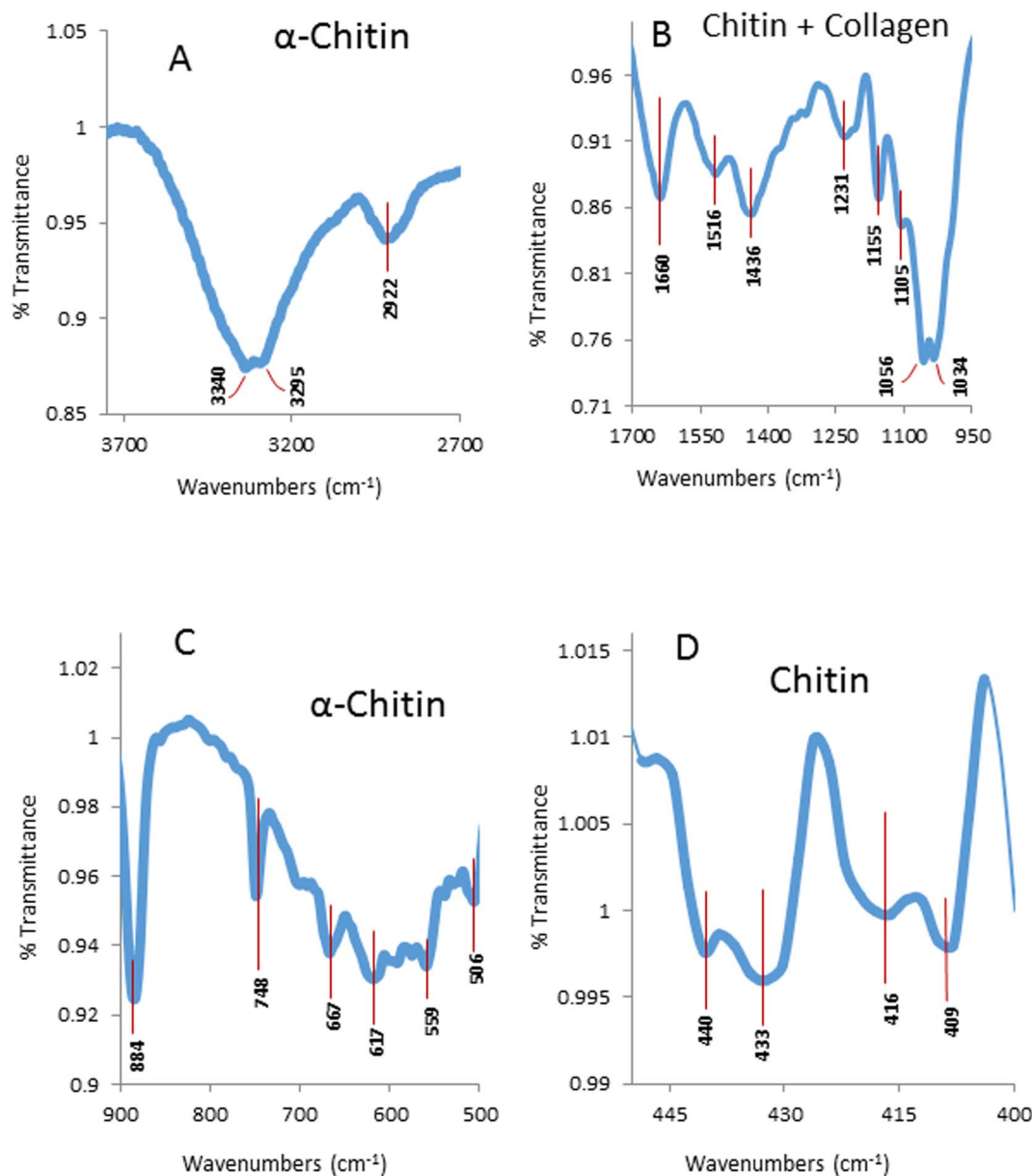


**Figure 5** | ATR-FTIR spectra of chitins in the insoluble organic matrix (IOM) fraction.

spectra were recorded from the lyophilized samples (Fig. 3B). As shown in Figure 3B, the FTIR spectra of chitin exhibited doublet peaks at 3340 and 3295  $\text{cm}^{-1}$  which can be assigned to N-H stretching (amide A). The main chitin band in IOM is present at 1660  $\text{cm}^{-1}$ . Another strong band attributed to chitin is visible in the range 1030–1110  $\text{cm}^{-1}$  (stretching C = O) at the doublet 1056 and 1034  $\text{cm}^{-1}$ . All FTIR spectra (667, 559, 506, 459, 433, 409  $\text{cm}^{-1}$ ) in the fingerprint region (400–700  $\text{cm}^{-1}$ ) again showed crystalline chitin<sup>4</sup>. However, the chitin of IOM in the fingerprint region is exhibiting a higher number of peaks with different wavenumbers positions. Like SOM, IOM attributed the same structural protein amide bands, amide A (3000–4000  $\text{cm}^{-1}$ ), amide B (2800–2990  $\text{cm}^{-1}$ ), amide I (1600–1700  $\text{cm}^{-1}$ ), amide II (1300–1590  $\text{cm}^{-1}$ ) and amide III (1200–1290  $\text{cm}^{-1}$ ). According to Fernandes et al.<sup>8</sup> the amide bands in IOM showed similar characterization as collagen-chitosan scaffolds. The main chitin bands on the structural crystalline side were amide A (3340, 3295  $\text{cm}^{-1}$ ), amide B (2922  $\text{cm}^{-1}$ ), amide I (1660  $\text{cm}^{-1}$ ), amide II (1436  $\text{cm}^{-1}$ ), and the amide III (1231  $\text{cm}^{-1}$ ). As shown in Fig. 5, structural position and intensity, especially in the fingerprint region of the IOM spectra were different than for the

SOM. To specify the chitin bands in the IOM fraction, FTIR spectra within each region were recorded separately (Fig. 5). One band in the CH stretching region of the IOM IR spectra at 2922  $\text{cm}^{-1}$  is characteristic of  $\alpha$ -chitin (Fig. 5A)<sup>30</sup>. The fingerprint region of the IR spectrum at 559  $\text{cm}^{-1}$  is also characteristic of  $\alpha$ -chitin (Fig. 5C)<sup>30</sup>.

Although spectral positions of chitins are similar in both fractions, the main differences of functional groups of detected chitin bands between SOM and IOM need to be understood. As mentioned above, the arrows in figure 6A, B indicate major differences between the two fractions. The three regions (Fig. 6A) define diagnostic regions of functional groups which might be mainly associated with the presence of proteins/lipids (R1), protein and polysaccharides (R2) and polysaccharides (R3).

**Bulk calcified skeletal material.** In order to understand the structural information of proteins and mineral composition in skeletal material of *C. compactum*, FTIR analysis was carried out. Figure 7 shows that the skeletons contain structural protein amide bands, named amide A (3000–3600  $\text{cm}^{-1}$ ), amide B (2800–2990  $\text{cm}^{-1}$ ), amide I & II (1300–1700  $\text{cm}^{-1}$ ), amide III (1200–1290  $\text{cm}^{-1}$ ). These bands

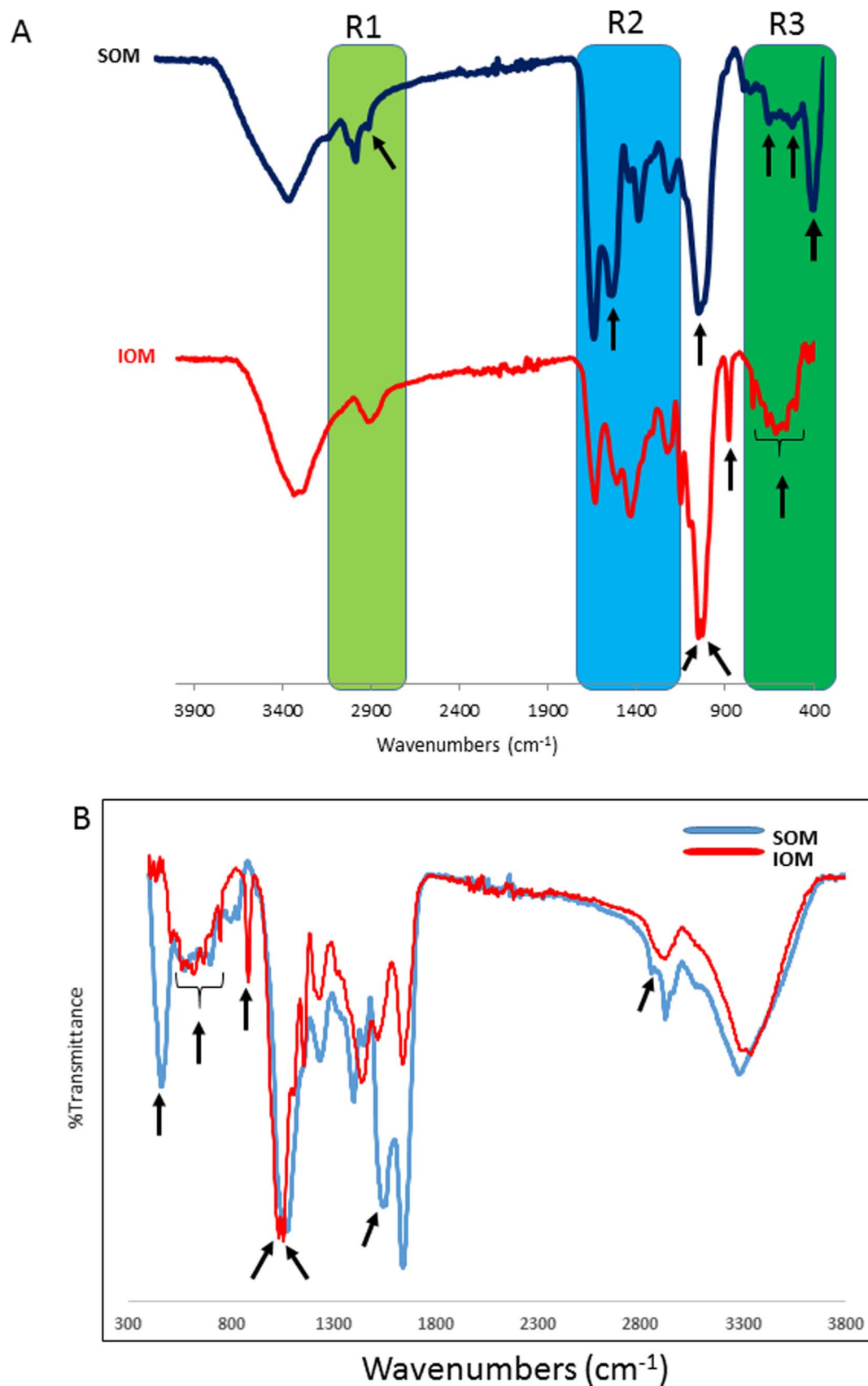


**Figure 6** | Comparison of detected chitin bands between SOM and IOM fractions. The arrows (A, B) indicate major differences between two fractions. Three regions (Fig. A) are diagnostic of functional groups showing the presence of proteins/lipids (R1), protein and polysaccharides (R2) and polysaccharides (R3).

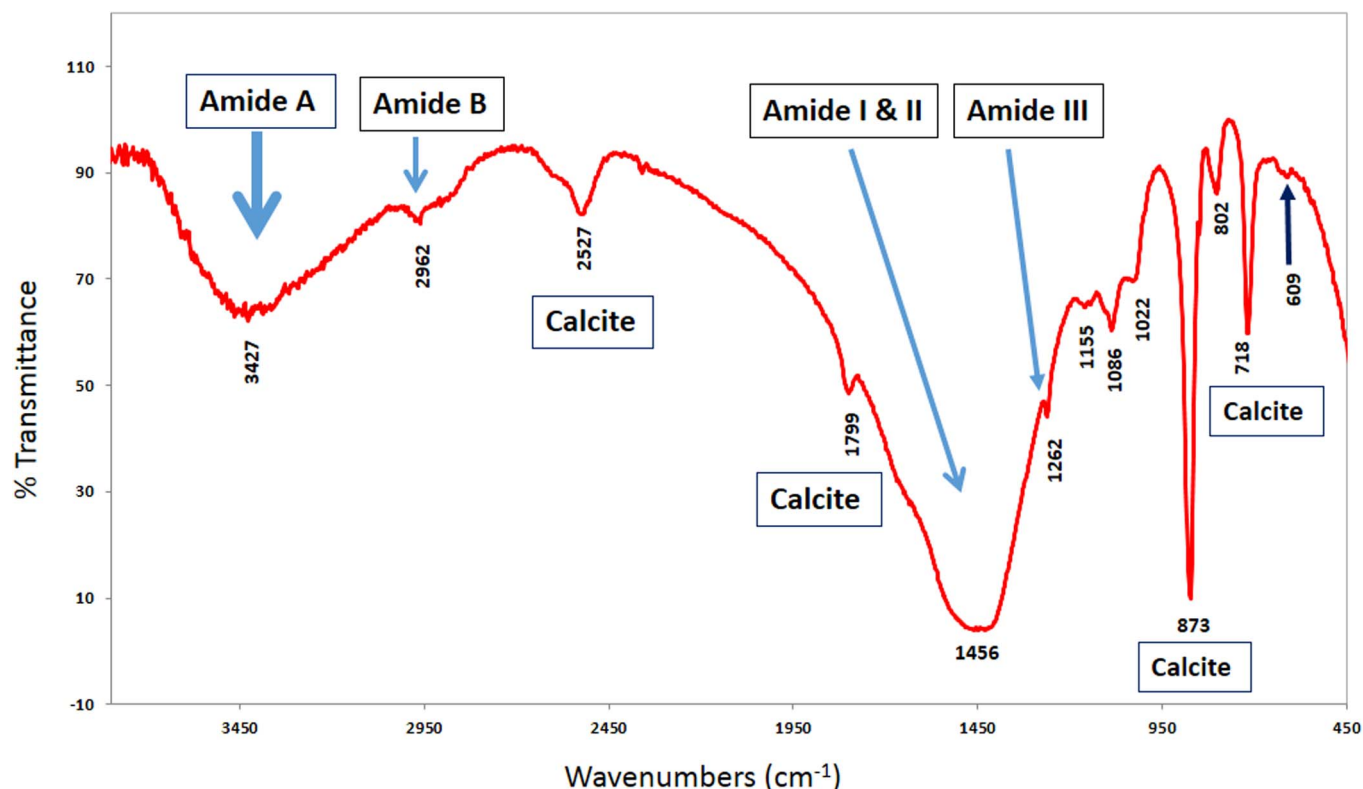


**Figure 7** | FTIR spectra of a bulk skeletal powder sample of *C. compactum* showing various conformations of molecules and the mineral compositions nucleated by chitin and collagen matrix molecules.

contain both chitins and collagen<sup>8,30</sup> and the crystallization of skeletal minerals might be controlled by these two polymers. The spectrum reveals two peaks at 2527 and 1799  $\text{cm}^{-1}$  which in shape and position are evidence for the presence of calcite<sup>31</sup>. Two strong Mg-calcite bands at 718  $\text{cm}^{-1}$  (v4) and 873  $\text{cm}^{-1}$  (v2) were also identified by FTIR<sup>32</sup>. The main chitin bands in the bulk skeletal structural crystalline side were amide A (3427  $\text{cm}^{-1}$ ), amide B (2962  $\text{cm}^{-1}$ ), amide I & II (1456  $\text{cm}^{-1}$ ), and the amide III (1262  $\text{cm}^{-1}$ ).

FTIR peaks in the SOM and IOM are at the same position in the bulk skeleton, which indicate two biopolymers (chitin and collagen) obtained in the purified organic matrices are significantly involved in the precipitation of  $\text{CaCO}_3$  in the skeleton (Fig. 8). The points of FTIR spectra with different colored boxes indicate the chitin and collagen matrix molecules eventually influence the formation of the algal skeletal structure by nucleating the original minerals in the calcification system (Figs. 1, 8). Purified SOM and IOM show chitin and collagen peaks in the same position region as in the bulk sample, which clearly demonstrates that chitin and collagen are involved in the calcification process.

**X-ray diffraction (XRD) of calcified skeletons.** To detect the orientation of crystal structures and understand the functional properties of the organic matrix components in the calcified skeletons of *C. compactum*, the finely ground skeletal powder samples were analyzed by XRD. The XRD pattern of the skeleton is shown in Fig. 9. The X-ray diffractational analysis revealed that the crystalline form of calcium carbonate in the algal skeletons was polycrystalline calcite and the structures designed in the skeletons were controlled by the organic matrix molecules. The main diffraction face intensity is the rhombohedra calcite at (104)  $2\theta = 29.5^\circ$  and the next to strongest faces are the calcites at [113], [110], [202], [116], [012], [122], [024], [211] and [006], respectively (Fig. 9). The diffraction angle,  $2\theta = 29.5^\circ$  in the calcite (104) indicates the

presence of Mg-calcite because the diffraction angle for pure calcite is at a maximum  $2\theta = 29.3^\circ$ <sup>29,33</sup>. The crystalline components in the sample exhibited the characteristic chitin and collagen bands in the calcite planes. Figure 9 shows the XRD pattern of different chitins ( $\alpha$ -chitins: 110,202, 012;  $\beta$ -chitin: 122)<sup>30,34</sup> and collagen bands (110, 211, 202).

## Discussion

Chitin, a naturally abundant polysaccharide and a supporting material of many marine calcifiers such as crustaceans<sup>2</sup>, is reinforced by calcium carbonate in association with proteins in nature to provide structural strength. Our study on this biomineralization process indicates that the protein-polysaccharide of the organic matrices such as chitin and collagen in Subarctic coralline algal skeletons plays a key role in stabilizing calcite crystals (Fig. 1, 7, 8). The structural characterization of chitin can be easily distinguished using vibrational spectroscopy because this structure is spectroscopically distinct and well documented<sup>3,7,10,14,31,34</sup>. To our knowledge, there are no published studies about the functions of chitin and collagen on the biomineralization of other coralline specimens; therefore, different marine organisms with different biominerals were used for comparison. In a recent review, the details of the elemental and organic influences (chitin and collagen) in carbonate systems were described<sup>3</sup>. The presence of chitin in the biomineralization system has been discussed in detail for different calcifiers<sup>1–3</sup>. One report indicated that the chitin is potentially involved in the formation of skeletons in calcifying marine sponges<sup>4</sup>. Therefore, our data are consistent with the basic concepts of the relationship between the crystal nucleus and its base planes with the organic matrices<sup>1–4</sup> produced in other calcifying marine organisms.

There are two principal skeletal systems which support the cellular structure of animal tissues: chitinous and collagenous frameworks<sup>5</sup>. It has been suggested that collagen in fungi which normally contain chitin<sup>35</sup> supports the cellular structure. The collagenous skeleton



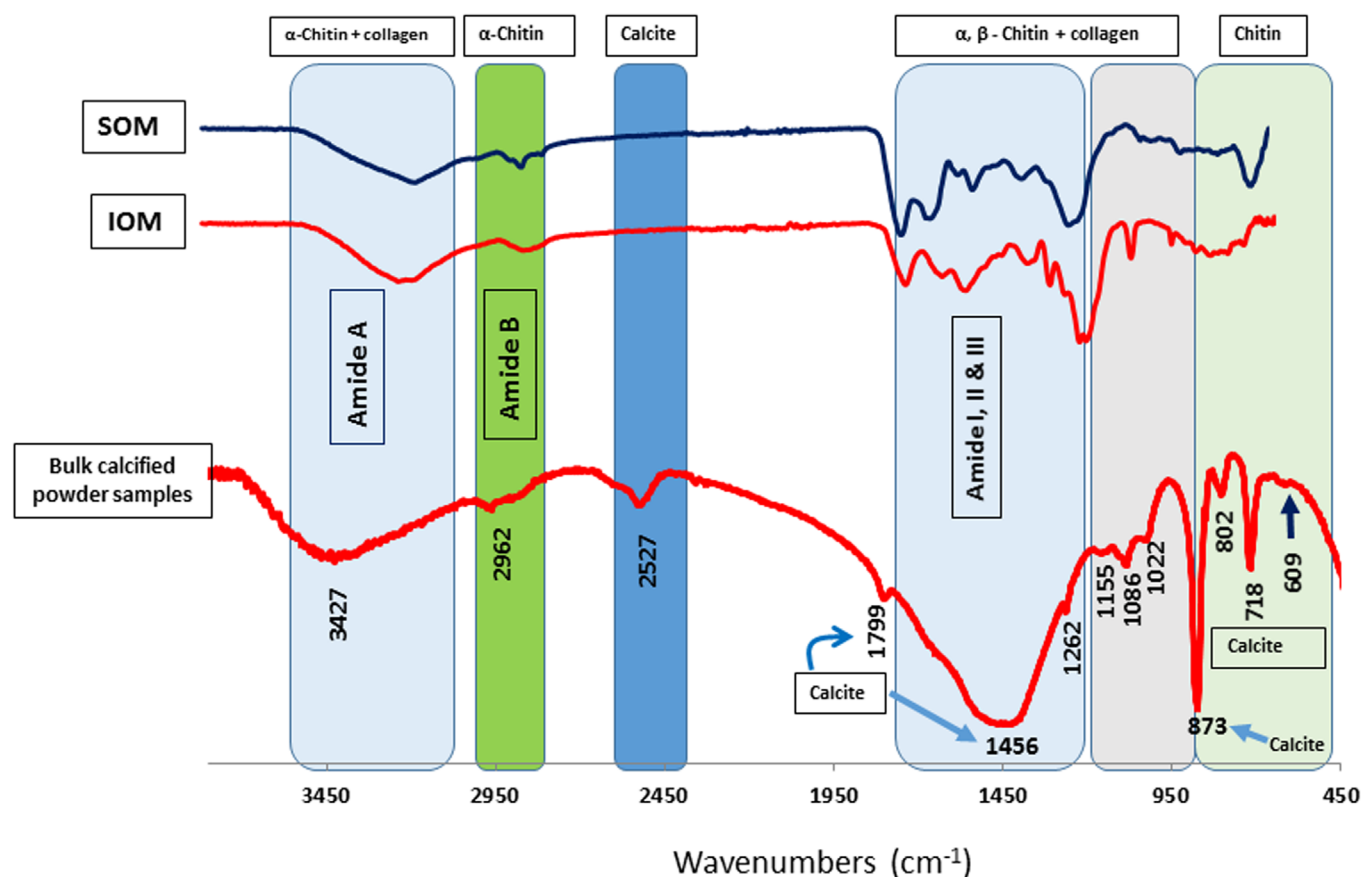


**Figure 8 | Structural comparison of FTIR spectra between organic matrix fractions (SOM and IOM) and the bulk skeletal powder.** Graphs for SOM, IOM fractions and bulk skeletal powder are indicated (see spectra for SOM and IOM in Fig. 2). Different colored boxes in the spectra indicate involvement of molecules in SOM and IOM fractions in forming skeletal structure in the calcification system.

consists principally of the unique fibrous protein collagen I, together with different quantities of non-collagenous proteins, while the chitinous system contains amino-polysaccharide chitin together with proteins<sup>36</sup>. The FTIR spectra of collagen in the range of 4000–400  $\text{cm}^{-1}$  show main absorption bands indicative of amide A (3333  $\text{cm}^{-1}$ ), amide B (2922  $\text{cm}^{-1}$ ), amide I (1653  $\text{cm}^{-1}$ ), amide II (1539  $\text{cm}^{-1}$ ), and the amide III (1238  $\text{cm}^{-1}$ )<sup>37</sup>. A free N-H stretching vibration commonly occurs in the range of 3400–3440  $\text{cm}^{-1}$ . The amide B peak of the collagens (2922  $\text{cm}^{-1}$ ) in IOM was attributed to the asymmetrical stretch of  $\text{CH}_2$  (2920–2922  $\text{cm}^{-1}$ ) stretching vibration (Fig. 3).

The chitin is strongly involved in different invertebrates and it can be regarded as the substrate that binds other macromolecules, which in turn induce nucleation of the mineral phase<sup>38</sup>. This is well described for mollusc shell nacre, where chitin is believed to be an important component of the molluscan organic matrix<sup>1</sup>. Chitin contributes the framework at the base of the biological hierarchy for calcification<sup>37</sup>. An alignment between the orientation of chitin fibres and the crystallographic axes of the mineral phase was observed in brachiopod and mollusc shells as well<sup>9,10</sup>. The chitin matrix was reported as the sole template for mineralization or in association with other molecules in the calcification system of several organisms<sup>31,39–41</sup>. Hall et al.<sup>39</sup> investigated the Mg-calcite *in vivo* in the Bryozoa skeletons, where chitin was the sole template in the calcification system.

The association of organic matrix components with biomineralized structures<sup>1,36,42</sup> and their observed effect on crystallization kinetics strongly suggest that these compounds modify the growth stage of minerals. This conclusion is reinforced by observations of faceted crystal surfaces in a number of cases, including the calcite crystals

reported by Mann<sup>43</sup>. On the other hand, many biomineralized structures in nature suggest that organic components also control nucleation. Moreover, there is a substantial body of evidence to suggest that proteins and other organic molecules serve as “templates”, providing preferential sites for nucleation and controlling the orientation of the resulting crystals<sup>29,44</sup>.

Our studies on the biomineralization process of the algal skeletons indicated that the organic matrix components associated with the chitin and collagen molecules play a crucial role in promoting

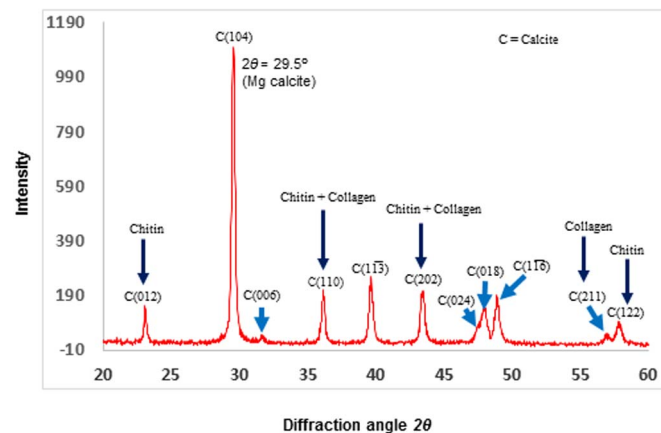


**Figure 9 | X-ray diffraction analysis of calcified skeletal powder samples of *C. compactum*.** The  $2\theta$  scan identifies the mineral form of calcium carbonate with calcitic crystal planes, which were nucleated by chitin and collagen matrices. Black arrows show the chitin and collagen bands.



and organizing mineral growth (Fig. 1). The purification of organic matrices and their complete spectroscopic analyses provide us with comprehensive data on the biomaterials contained within the skeletons of coralline algae. These results have revealed that the organic matrix of the alga *C. compactum* is composed of two important natural biopolymers, chitin and collagen, and these are mainly responsible for the formation of Mg-calcite in the algal skeletons. Nash et al.<sup>14</sup> showed that a high magnesium mineral (dolomite) in some tropical coralline algae can protect them from ocean acidification. Therefore, the chitin containing polysaccharides described here might be key organic matrix molecules in the calcification process to make *C. compactum* less susceptible to the negative impacts of ocean acidification. Chitin provides additional strength to the calcified algal skeleton and therefore protection from the destructive actions of grazing or wave tool impacts. Grazing on coralline algae is a natural process, and in fact needed to provide a photosynthetic surface clear of fleshy algal overgrowth. *C. compactum* has developed a protective calcified surface layer, the so-called epithallium that shields the underlying skeleton from physical grazing damage<sup>12,45</sup>. However, with increasing rates of ocean acidification and a declining ability to calcify, the algal skeleton might be weakened in the absence of the strengthening effect of chitin and become more susceptible to destruction by grazing. A deeply grazed *Clathromorphum* crust would quickly bioerode and lose its ecosystem function of harbouring a highly diverse species association<sup>12,46</sup>. Given the fact that *Clathromorphum* corallines encrust a spatially significant portion of shallow rocky substrate throughout the entire Arctic and Subarctic<sup>12</sup> a change in its abundance would significantly affect high-latitude shallow marine ecosystems. In summary, the results obtained from this study not only further our understanding of the complex structure of coralline algal skeletons, but also demonstrate an effective analytical approach to study biological materials in coralline algae.

Coralline algae incorporate organic materials into their skeletons that provide a chitin matrix for mineral formation, but how their nucleation occurs in the biomineralization system and how they shape or organize their skeletal crystals remains an unresolved question. This is the first study confirming the presence of chitin as an endogenous material within the structural tissues of coralline algae. This new finding therefore contributes to elucidating the coralline algal calcification process.

- Mann, S. Molecular Recognition in Biomineralization. *Nature* **332**, 119–124 (1988).
- Kurita, K. Chitin and chitosan: functional biopolymers from marine crustaceans. *Mar Biotechnol* (NY) **8**, 203–226, doi:10.1007/s10126-005-0097-5 (2006).
- Ehrlich, H. Chitin and collagen as universal and alternative templates in biomineralization. *Int Geol Rev* **52**, 661–699, doi:10.1080/00206811003679521 (2010).
- Ehrlich, H. et al. First evidence of the presence of chitin in skeletons of marine sponges. Part II. Glass sponges (Hexactinellida: Porifera). *J of Exp Zool. Part B, Mol and develop evol* **308**, 473–483, doi:10.1002/jez.b.21174 (2007).
- Rinaudo, M. Chitin and chitosan: Properties and application. *Prog in poly Sci* **31**, 603–632 (2006).
- Brugnerotto, J. et al. An infrared investigation in relation with chitin and chitosan characterization. *Polymer* **42**, 3569–80 (2001).
- Tan, W., Krishnaraj, R. & Desai, T. A. Evaluation of nanostructured composite collagen--chitosan matrices for tissue engineering. *Tissue Eng* **7**, 203–210, doi:10.1089/107632701300062831 (2001).
- Fernandes, L. L. Cytocompatibility of Chitosan and Collagen-Chitosan Scaffolds for Tissue Engineering. *Polimeros* **21**, 1–6 (2011).
- Banks, I. R. et al. A chitin synthase and its regulator protein are critical for chitosan production and growth of the fungal pathogen *Cryptococcus neoformans*. *Eukaryot Cell* **4**, 1902–1912, doi:10.1128/EC.4.11.1902-1912.2005 (2005).
- Sendbusch, P. V. <http://www.biologie.uni-hamburg.de/b-online/e26/26d.htm>, Botany Online: Cell Walls of Algae., (2003) Date of access: 29/10/2007.
- Lipke, P. N. & Ovalle, R. Cell wall architecture in yeast: new structure and new challenges. *J Bacteriol* **180**, 3735–3740 (1998).
- Adey, W. H., Halfar, J. & Williams, B. The coralline genus *Clathromorphum* fossil emend. adey: biological, physiological, and ecological factors controlling carbonate production in an arctic-subarctic climate archive. *Smithsonian Contributions to the Marine Sciences* **40**, 1–41 (2013).
- Kamenos, N. A. et al. Coralline algal structure is more sensitive to rate, rather than the magnitude, of ocean acidification. *Glob Chang Biol* **19**, 3621–3628, doi:10.1111/gcb.12351 (2013).
- Nash, et al. Dolomite-rich coralline algae in reefs resist dissolution in acidified condition. *Nat clim change* **3**, 268–272 (2013).
- Kuffner, I. B. A., A. J. & JOKIEL, P. Decreased abundance of crustose coralline algae due to ocean acidification. *Nat Geosci* **1**, 114–117 (2008).
- Ragazzola. Ocean acidification weakens the structural integrity of coralline algae. *Glob Change Biol* **18**, 2804–2812 (2012).
- Martin, S. & Gattuso, J.-P. Response of Mediterranean coralline algae to ocean acidification and elevated temperature. *Glob Change Biol* **15**, 2089–2100 (2009).
- Büdenbender, J., Riebesell, U. & Form, A. Calcification of the Arctic coralline red alga *Lithothamnion glaciale* in response to elevated CO<sub>2</sub>. *Mar Ecol Prog Series* **441**, 79–87 (2011).
- Ries, J. B. Aragonitic Algae in calcite seas: Effect of sea water Mg/Ca ratio on algal sediment production. *J Sediment Res* **76**, 515–523 (2006).
- Halfar, J. et al. Arctic sea-ice decline archived by multicentury annual-resolution record from crustose coralline algal proxy. *Proc Natl Acad Sci U S A* **110**, 19737–19741, doi:10.1073/pnas.1313775110 (2013).
- Kamenos, N. A. North Atlantic summers have warmed more than winters since 1353, and the response of marine zooplankton. *Proc Natl Acad Sci U S A* **107**, 22442–22447, doi:10.1073/pnas.1006141107 (2010).
- Kamenos, N. A. et al. Coralline algae are global palaeothermometers with bi-weekly resolution. *Geochim Cosmochim Acta* **72**, 771–779 (2008).
- Kamenos, N. A. et al. Reconstructing Greenland ice sheet runoff using coralline algae. *Geology* **40**, 1095–1098 (2012).
- Darrenougue, N. et al. Growth and chronology of the rhodolith-forming, coralline red alga *Sporolithon durum*. *Mar Ecol Prog Series* **474**, 105–119 (2013).
- Wanamaker, A. D., Hetzinger, S. & Halfar, J. Reconstructing mid- to high-latitude marine climate and ocean variability using bivalves, coralline algae, and marine sediments from the Northern Hemisphere. *Palaeogeogr, Palaeoclim, Palaeoecol* **302**, 1–9 (2011).
- Teichert, S. et al. Rhodolith beds (Corallinales, Rhodophyta) and their physical and biological environment at 80°31'N in Nordkappbukta (Nordaustlandet, Svalbard Archipelago, Norway). *Phycologia* **51**, 371–390 (2012).
- Adey, W. H. & Macintyre, I. G. Crustose coralline algae: A re-evaluation in the geological sciences. *Geol Soc Am Bull* **84**, 883–904 (1973).
- Rahman, M. A., Isa, Y., Takemura, A. & Uehara, T. Analysis of proteinaceous components of the organic matrix of endoskeletal sclerites from the alcyonarian *Lobophytum crassum*. *Calcif Tissue Int* **78**, 178–185, doi:DOI 10.1007/s00223-005-0253-y (2006).
- Rahman, M. A., Oomori, T. & Worheide, G. Calcite formation in soft coral sclerites is determined by a single reactive extracellular protein. *J Biol Chem* **286**, 31638–31649, doi: 10.1074/jbc.M109.070185 (2011).
- Cárdenas, G., Cabrera, G., Taboada, E. & Miranda, S. P. Chitin characterization by SEM, FTIR, XRD, and <sup>13</sup>C cross polarization/mass angle spinning NMR. *J Appl Polym Sci* **93**, 1876–85 (2004).
- Mikkelsen, A., Engelsen, S. B., Hansen, H. C. B., Larsen, O. & Skibsted, L. H. Calcium carbonate crystallization in the alpha-chitin matrix of the shell of pink shrimp, *Pandalus borealis*, during frozen storage. *J Cryst Growth* **177**, 125–134 (1997).
- Rahman, M. A. & Oomori, T. In Vitro Regulation of CaCO<sub>3</sub> Crystal Growth by the Highly Acidic Proteins of Calcitic Sclerites in Soft Coral, *Sinularia polydactyla*. *Connect Tissue Res* **50**, 285–293, doi:10.3109/03008200802714933 (2009).
- Rahman, M. A. & Oomori, T. Structure, crystallization and mineral composition of sclerites in the alcyonarian coral. *J Cryst Growth* **310**, 3528–3534, doi:10.1016/j.jcrysgro.2008.04.056 (2008).
- Zhang, Y., Xue, C., Xue, Y., Gao, R. & Zhang, X. Determination of the degree of deacetylation of chitin and chitosan by X-ray powder diffraction. *Carbohydr Res* **340**, 1914–1917, doi:10.1016/j.carres.2005.05.005 (2005).
- Celerin, M. et al. Fungal fimbriae are composed of collagen. *EMBO J* **15**, 4445–4453 (1996).
- Friess, W. & Lee, G. Basic thermoanalytical studies of insoluble collagen matrices. *Biomaterials* **17**, 2289–2294 (1996).
- Feng, W. et al. Optimization of enzyme-assisted extraction and characterization of collagen from Chinese sturgeon (*Acipenser sturio* Linnaeus) skin. *Pharmacog mag* **9**, S32–37, doi:10.4103/0973-1296.117859 (2013).
- Weiss, I. M. & Schönlitzer, V. The distribution of chitin in larval shells of the bivalve mollusk *Mytilus galloprovincialis*. *J Struct Biol* **153**, 264–277, doi:10.1016/j.jsb.2005.11.006 (2006).
- Hall, S. R., Taylor, P. D., Davis, S. A. & Mann, S. Electron diffraction studies of the calcareous skeletons of bryozoans. *J Inorg Biochem* **88**, 410–419 (2002).
- Falini, G., Fermani, S. & Ripamonti, A. Oriented crystallization of octacalcium phosphate into beta-chitin scaffold. *J Inorg Biochem* **84**, 255–258 (2001).
- Falini, G., Fermani, S. & Ripamonti, A. Crystallization of calcium carbonate salts into beta-chitin scaffold. *J Inorg Biochem* **91**, 475–480 (2002).
- Falini, G., Albeck, S., Weiner, S. & Addadi, L. Control of aragonite or calcite polymorphism by mollusk shell macromolecules. *Science* **271**, 67–69 (1996).
- Mann, S. *Biomineralization: Principles and concepts in Bioinorganic Materials Chemistry* (Oxford Univ. Press, New York, 2001).



44. Wheeler, A. P., George, J. W. & Evans, C. A. Control of calcium carbonate nucleation and crystal growth by soluble matrix of oyster shell. *Science* **212**, 1397–1398, doi: 10.1126/science.212.4501.1397 (1981).
45. Steneck, R. S. A limpet-coralline alga association: Adaptations and defenses between a selective herbivore and its prey. *Ecology* **63**, 507–522 (1982).
46. Chenelot, H., Jewett, S. C. & Hoberg, M. K. Macrobenthos of the nearshore Aleutian Archipelago, with emphasis on invertebrates associated with *Clathromorphum nereostratum* (Rhodophyta, Corallinaceae). *Mar Biodiversity* **41**, 413–424 (2011).

## Acknowledgments

Funding to J.H. was provided by the Natural Sciences and Engineering Research Council of Canada and a Canadian Foundation for Climate and Atmospheric Sciences Grant.

## Author contributions

M.A.R. performed the experiments; J.H. and M.A.R. wrote the manuscript.

## Additional information

**Competing financial interests:** The authors declare no competing financial interests.

**How to cite this article:** Rahman, M.A. & Halfar, J. First evidence of chitin in calcified coralline algae: new insights into the calcification process of *Clathromorphum compactum*. *Sci. Rep.* **4**, 6162; DOI:10.1038/srep06162 (2014).



This work is licensed under a Creative Commons Attribution-NonCommercial-NoDerivs 4.0 International License. The images or other third party material in this article are included in the article's Creative Commons license, unless indicated otherwise in the credit line; if the material is not included under the Creative Commons license, users will need to obtain permission from the license holder in order to reproduce the material. To view a copy of this license, visit <http://creativecommons.org/licenses/by-nc-nd/4.0/>